COMPEL - The international journal for computation and mathematics in electrical and electronic engineering

Numerical modeling of a MEMS actuator considering several magnetic force calculation methods

Thomas Preisner, Christian Bolzmacher, Andreas Gerber, Karin Bauer, Eckhard Quandt, Wolfgang Mathis,

Numerical modeling of a MEMS actuator considering several magnetic force calculation methods

Thomas Preisner, Christian Bolzmacher, Andreas Gerber, Karin Bauer, Eckhard Quandt and Wolfgang Mathis
(The authors' affiliations can be found at the end of the article.)

Abstract

Purpose – The purpose of this paper is to investigate the accuracy of different force calculation methods and their impact on mechanical deformations. For this purpose, a micrometer scaled actuator is considered, which consists of a micro-coil and of a permanent magnet (PM) embedded in a deformable elastomeric layer.

Design/methodology/approach – For the magnetic field evaluation a hybrid numerical approach (finite element method/boundary element method (FEM/BEM) coupling and a FEM/BEM/Biot-Savart approach) is used, whereas FEM is implemented for the mechanical deformation analysis. Furthermore, for the magneto-mechanical coupling several force calculation methods, namely the Maxwell stress tensor, the virtual work approach and the equivalent magnetic sources methods, are considered and compared to each other and to laboratory measurements.

Findings – The numerically evaluated magnetic forces and the measured ones are in good accordance with each other with respect to the normal force acting on the PM. Nevertheless, depending on the used method the tangential force components differ from each other, which leads to slightly different mechanical deformations.

Research limitations/implications – Since the force calculations are compared to measurement data, it is possible to give a suggestion about their applicability. The mechanical behavior of the actuator due to the acting forces is solely calculated and therefore only an assumption concerning the deformation can be given.

Originality/value – A new kind of micrometer scaled actuator is numerically investigated by using two different hybrid approaches for the magnetic field evaluation. Based on those, the results of several force calculation methods are compared to measurement data. Furthermore, a subsequent structural analysis is performed, which shows slightly different mechanical deformations depending on the used force calculation method.

Keywords Actuators, MEMS, Force measurement

Paper type Research paper

1. Introduction

Fluid flow may be manipulated by wall motion, induced wall temperature variations and fluid mass injection using macro scale devices (Hefner and Bushell, 1990). Micro-electro-mechanical systems (MEMS) actuators are a good choice for local fluid flow manipulation in very thin boundary layers where high operational frequencies and spatial resolution are required. An example application is the delay of

This work was financially supported by the German Federal Ministry of Education and Research (BMBF, contract 13N8975).

COMPEL: The International Journal for Computation and Mathematics in Electrical and Electronic Engineering
Vol. 30 No. 4, 2011
pp. 1176-1188

0332-1649
DOI 10.1108/03321641111133118

laminar-turbulent transition (that comes along with a significant reduction of skin friction drag) by active wave cancellation by superimposition of an artificially generated counter wave, which is induced by these actuators.

Many actuation technologies have been proposed for MEMS devices, including piezoelectric, electrostatic, thermo pneumatic, electrochemical, shape memory alloy, and electromagnetic principles. Generally, electrostatic and piezoelectric interactions require large driving voltages. Thermo pneumatic, electrochemical and shape memory alloy devices show only small bandwidth, whereas magnetic actuation potentially provides both, large force and large displacement in an energy efficient manner (Liu, 1998).

The considered MEMS actuator in this study is applicable for aeronautic applications and consists of a thin micrometer coil and a permanent magnet (PM), which are separated by an elastomer (Figure 1(a)). The elastomer acts as a filling medium between the coil and the PM and protects the coil against external impacts. Furthermore, the PM is embedded in another elastomeric layer. The stiffness of both elastomeric layers may be adapted to different application requirements such as frequency behavior or displacement amplitude.

In this work, the described MEMS actuator is numerically investigated. The study is focused on a hybrid finite element method/boundary element method (FEM/BEM) and different force calculation methods, which are compared to each other and to laboratory measurements. Furthermore, depending on these results, the impact on the mechanical deformation of the elastomeric layers is numerically analyzed. Moreover, all results are compared to an alternative approach, whereas the magnetic field inducing micro-coil is calculated with the Biot-Savart integral equation.

2. Hybrid numerical formulation

The intention of this work was the optimization of the spacious amplitude and therewith the acting forces due to the magnetic interaction of the PM and the current carrying micro-coil. To simplify matters, the described configuration is considered in a magnetostatic point of view and the FEM is applied to calculate the occurring magnetic interaction. While FEM has for instance, the advantages in modeling heterogeneous materials in a bounded domain, it is not applicable to the field evaluation of an unbounded one. In order to overcome this disadvantage and particularly, to neglect the influences of improper boundary conditions, the BEM is coupled to the FEM. The considered calculation domain is, therefore, decomposed into two parts $\Omega = \Omega_F \cup \Omega_B$ (Figure 1(b)). Therefore, the model problem is defined as follows:

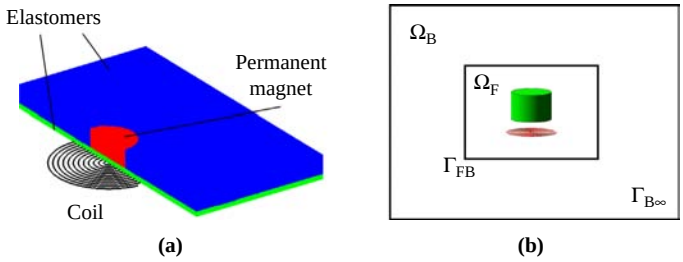

Figure 1.
(a) The model configuration of the MEMS actuator and (b) the decomposed calculation domain

$$\nabla \times \frac{1}{\mu}(\nabla \times \mathbf{A}) - \nabla \frac{1}{\mu}\nabla \cdot \mathbf{A} - \nabla \times \frac{\mu_0}{\mu}\mathbf{M} - \mathbf{J} = 0 \quad \text{in } \Omega_F \tag{1}$$

$$\nabla^2 \mathbf{A} = 0 \quad \text{in } \Omega_B, \tag{2}$$

where $\mathbf{A}$ is the magnetic vector potential, $\mathbf{J}$ is the current density, $\mathbf{M}$ is the magnetization, μ is the material permeability and μ_0 is the permeability of free space. The so-called penalty term $-\nabla 1/\mu \nabla \cdot \mathbf{A}$ in equation (1) indirectly enforces the Coulomb gauge and improves in a finite element approach the numerical stability of the solution of the coupled system of equations (Preis *et al.*, 1991). Furthermore, the following boundary conditions are set:

$$\mathbf{A} = \textit{continuous} \quad \text{on } \Gamma_{FB} \tag{3}$$

$$\frac{\partial \mathbf{A}}{\partial n_F} = -\frac{\partial \mathbf{A}}{\partial n_B} \quad \text{on } \Gamma_{FB} \tag{4}$$

$$\mathbf{A} = \mathbf{0} \quad \text{on } \Gamma_{B\infty}, \tag{5}$$

whereas the minus sign in equation (4) corresponds to the orientation of the normal vector at the interface on Γ_{FB}. By applying the method of weighted residuals to equation (1), using Gauss's law and making some mathematical transformations, the following weak formulation can be obtained:

$$\begin{aligned} &\int_{\Omega_F} \left[(\nabla \times \mathbf{A}) \cdot (\nabla \times \mathbf{N}) + \frac{1}{\mu}(\nabla \cdot \mathbf{A})(\nabla \cdot \mathbf{N}) \right] d\Omega_F \\ &\quad - \int_{\Gamma_{FB}} \left[\mathbf{N} \times \left(\frac{1}{\mu} \nabla \times \mathbf{A} \right) - \left(\frac{1}{\mu} \nabla \cdot \mathbf{A} \right) \mathbf{N} \right] d\boldsymbol{\Gamma}_{FB}, \\ &= \int_{\Omega_F} \left[\frac{\mu_0}{\mu} \mathbf{M} \cdot (\nabla \times \mathbf{N}) + \mathbf{N} \cdot \mathbf{J} \right] d\Omega_F - \int_{\Gamma_{FB}} \mathbf{N} \times \frac{\mu_0}{\mu} \mathbf{M} d\boldsymbol{\Gamma}_{FB} \end{aligned} \tag{6}$$

where $\mathbf{N}$ is the vector weighting function. After applying the Galerkin method to the weak formulation the following matrix equation can be set up (Kurz and Russenschuck, 1999):

$$\begin{pmatrix} [\mathbf{K}_{\Omega\Omega}] & [\mathbf{K}_{\Omega\Gamma}] & 0 \\ [\mathbf{K}_{\Gamma\Omega}] & [\mathbf{K}_{\Gamma\Gamma}] & [\mathbf{R}] \end{pmatrix} \begin{pmatrix} \mathbf{A}_\Omega \\ \mathbf{A}_\Gamma \\ \mathbf{Q}_\Gamma \end{pmatrix} = \begin{pmatrix} \mathbf{b} \\ 0 \end{pmatrix}, \tag{7}$$

where $[\mathbf{K}]$ and $[\mathbf{R}]$ are the stiffness and boundary matrices, respectively. The subscripts Ω and Γ represent the contributions of elements inside Ω_F and of elements, which are located at the boundary Γ_{FB}. The grouped vectors $\mathbf{A}_\Omega$, $\mathbf{A}_\Gamma$ and $\mathbf{Q}_\Gamma$ contain the magnetic vector potentials and their normal derivatives, while $\mathbf{b}$ represents the values corresponding to the right-hand side of equation (6).

In the second unbounded domain Ω_B, the BEM is used to solve equation (2). For this purpose, the method of weighted residuals is again used and applied to equation (2). By using the second Green's theorem the following formulation can be obtained:

$$\int_{\Omega_B} \nabla^2 \boldsymbol{\omega} \cdot \mathbf{A} d\Omega_B + \int_{\Gamma_{FB}} \boldsymbol{\omega} \mathbf{Q} d\Gamma_{FB} - \int_{\Gamma_{FB}} \mathbf{A} \frac{\partial \boldsymbol{\omega}}{\partial n} d\Gamma_{FB} = 0, \tag{8}$$

where $\mathbf{Q}$ is the normal derivative of $\mathbf{A}$. The weighting function $\boldsymbol{\omega}$ represents the fundamental solution of the Laplacian in 3D, which is given by:

$$u^*(\mathbf{r}, \tilde{\mathbf{r}}) = \frac{1}{4\pi} |\mathbf{r} - \tilde{\mathbf{r}}|^{-1}. \tag{9}$$

With equation (9) and $q^* = \partial u^* / \partial n$, equation (8) leads to the following expression (Kurz *et al.*, 1995):

$$c(\mathbf{r})\mathbf{A}(\mathbf{r}) - \int_{\Gamma_{FB}} u^*(\mathbf{r}, \tilde{\mathbf{r}}) \mathbf{Q} d\Gamma_{FB} + \int_{\Gamma_{FB}} q^*(\mathbf{r}, \tilde{\mathbf{r}}) \mathbf{A} d\Gamma_{FB} = 0, \tag{10}$$

where the function $c(\mathbf{r})$ contains the interior solid angle at $\mathbf{r}$.

Now the boundary Γ_{FB} can be subdivided in m elements, so that the integral equation (10) can be transformed into a matrix formulation:

$$[\mathbf{H}]\mathbf{A}_\Gamma - [\mathbf{G}]\mathbf{Q}_\Gamma = 0. \tag{11}$$

In order to exploit the above-mentioned advantages of both numerical methods, the boundary conditions in equation (3) and equation (4) are used to set up the whole coupled system of equations (Preisner and Mathis, 2009):

$$\begin{pmatrix} [\mathbf{K}_{\Omega\Omega}] & [\mathbf{K}_{\Omega\Gamma}] & 0 \\ [\mathbf{K}_{\Gamma\Omega}] & [\mathbf{K}_{\Gamma\Gamma}] & [\mathbf{R}] \\ 0 & [\mathbf{H}] & [\mathbf{G}] \end{pmatrix} \begin{pmatrix} \mathbf{A}_\Omega \\ \mathbf{A}_\Gamma \\ \mathbf{Q}_\Gamma \end{pmatrix} = \begin{pmatrix} \mathbf{b} \\ 0 \\ 0 \end{pmatrix}. \tag{12}$$

As it was mentioned in the introduction, for this considered multiscale problem with a thin micro-coil and a relative large PM, it could be useful not to approximate the coil with finite elements, but rather calculate the magnetic coil field with the Biot-Savart integral equation and to obtain the whole magnetic field by the superposition of both results. By applying this FEM/BEM/Biot-Savart approach, the current density $\mathbf{J}$ in equation (6) has to be neglected.

3. Magnetic forces

After a precise magnetic field evaluation with the described hybrid FEM/BEM approach, a further challenge for a theoretical description of the micrometer scaled actuator is to compute the occurring forces due to the magnetic interaction. Up until now, force calculation methods and their improvement in accuracy and straightforward implementation are still a topic of interest in research. In this study, several commonly used magnetic force calculation methods, namely the Maxwell stress tensor (MST), the virtual work (VW) approach and the equivalent magnetic sources methods, are considered and compared to each other and to laboratory measurements. In order to almost complete the list of force calculation methods a few other studies should be noted here, which use the Korteweg-Helmholtz force density and the Kelvin force density

(Melcher, 1981; Lee *et al.*, 2000). Furthermore, an approach based on continuum sensitivity analyses using Lagrange multipliers is demonstrated in Kim *et al.* (2005).

3.1 Maxwell stress tensor

Considering the classical approach for the MST, the ferromagnetic material in the region of interest could be replaced by a distribution of currents in such a manner that the external field is not altered (Salon *et al.*, 1995). Based on this approach, the following tensor $\mathbf{T}$ can be derived:

$$\mathbf{T} = \frac{1}{\mu_0}\begin{bmatrix} B_x^2 - \frac{1}{2}|\mathbf{B}|^2 & B_xB_y & B_xB_z \\ B_yB_x & B_y^2 - \frac{1}{2}|\mathbf{B}|^2 & B_yB_z \\ B_zB_x & B_zB_y & B_z^2 - \frac{1}{2}|\mathbf{B}|^2 \end{bmatrix}. \tag{13}$$

The total force can then be computed by a volume integral of the divergence of the MST or by applying the divergence theorem and solving the integral equation over an enclosed surface:

$$\mathbf{F} = \int_{\Omega} \nabla \cdot \mathbf{T} d\Omega = \int_{\Gamma} \mathbf{T} d\mathbf{\Gamma}. \tag{14}$$

3.2 Virtual work principle

The VW principle is based on the energy law and the principle of a virtual displacement of the considered body (Coulomb, 1983). Then, the total magnetic force can be calculated by the derivation of the magnetic energy or co-energy, while keeping the flux or current constant. For a PM the energy formulation can be expressed as:

$$W = \frac{1}{2\mu_0}\int_{\Omega} (\mathbf{B} - \mathbf{B}_r) \cdot (\mathbf{B} - \mathbf{B}_r) d\Omega, \tag{15}$$

where $\mathbf{B}_r$ is the remanent induction.

In this work, another approach based on the idea presented in (de Medeiros *et al.*, 1998) was implemented. It is suggested that in a theoretical consideration the total force solution can be decomposed into two different parts, the intrinsic and the interaction forces. The evaluation of the intrinsic forces can normally not be accomplished by derivating equation (15), because the energy considered for that purpose, which is the stored energy due to the magnetization process, is incorrectly described with this equation. Contrary to the evaluation of the intrinsic forces, the interaction forces, which occurred due to an external magnetic field, can be calculated by derivating the interaction energy, which is well described by equation (15), while a linear rigid model can be assumed for the PM. To consider finally only the interaction forces, the intrinsic ones have to be withdrawn from the whole force solution. Concerning this matter in a finite element approach and derivating the intrinsic and the whole energy in a direction i, the interaction force in this direction at a node k can be obtained by solving the following equation:

$$F_{\text{interaction},ik} = F_{ik} - F_{\text{intrinsic},ik}$$
$$= \sum_{e_k} \left[\int_{\Omega_{e_k}} \frac{(\mathbf{B} - \mathbf{B}_r)}{\mu_0} \Im^{-1} \frac{\delta \Im}{\delta s_i} \mathbf{B} |\Im| d\Omega_{e_k} \right.$$
$$- \int_{\Omega_{e_k}} \frac{(\mathbf{B}_{air} - \mathbf{B}_r)}{\mu_0} \Im^{-1} \frac{\delta \Im}{\delta s_i} \mathbf{B}_{air} |\Im| d\Omega_{e_k}, \tag{16}$$
$$\left. + \int_{\Omega_{e_k}} \frac{\mathbf{B} \cdot (2\mathbf{B}_r - \mathbf{B})}{2\mu_0} \frac{\delta |\Im|}{\delta s_i} d\Omega_{e_k} - \int_{\Omega_{e_k}} \frac{\mathbf{B}_{air} \cdot (2\mathbf{B}_r - \mathbf{B}_{air})}{2\mu_0} \frac{\delta |\Im|}{\delta s_i} d\Omega_{e_k} \right],$$

where $\mathbf{B}_{air}$ is the magnetic induction of the single magnet in air, $\Im$ is the Jacobian and $|\Im|$ is the Jacobian determinant.

3.3 Equivalent magnetic sources

Further methods for calculating magnetic forces are the so-called equivalent magnetic sources methods. The idea is to replace the magnetization of a PM with equivalent magnetic currents or fictive magnetic charges (Kabashima *et al.*, 1988). Both approaches are separated into a volume and a surface current density (M-currents) or a volume and a surface charge density (M-charges):

$$\mathbf{J}_v = \nabla \times \mathbf{M} \quad \wedge \quad \mathbf{J}_s = -\mathbf{n} \times \mathbf{M} \tag{17}$$

$$\rho_v = -\mu_0 \nabla \cdot \mathbf{M} \quad \wedge \quad \rho_s = \mu_0 (\mathbf{n} \cdot \mathbf{M}). \tag{18}$$

If $\mathbf{M}$ is constant, the volume current density or rather the volume charge density vanishes and the occurring force densities can be calculated with the following expressions:

$$\mathbf{f}_s = \mathbf{J}_s \times \mathbf{B}_s \tag{19}$$

$$\mathbf{f}_s = \rho_s \mathbf{H}_s. \tag{20}$$

4. Actuator fabrication

The coils are fabricated by galvanic micro machining, except for the sputtered galvanic seed-layers (Cr/Au), on a 25 μm thick Kapton® substrate. First, the 8-10 μm thick lower Au windings and the 10 μm high vertical interconnect accesses (VIAs) are deposited. In order to fill the gaps between the lower windings and to electrically isolate the windings, a planarization step was required. To obtain a sufficient planarization degree (DOP $>$ 90 percent), a spin-coated benzocyclobutene (BCB) 4026-46 resin from Dow Chemical Company – cured at 150°C for 60 min in N_2 was used. Thinning out the BCB layer was accomplished by a reactive ion etching (RIE) process using a SF_6 (25 percent)/O_2 (75 percent) gas-mixture. Then, the wire connection is applied by electro deposition. For instance, in Figure 2, two fabricated examples of coils with $N = 6$ and $N = 13$ windings are shown. After completion of the coil manufacturing, the actuator is assembled. The intermediate elastomeric layer is applied by spin coating after electrical connection of the coil in order to obtain a homogeneous thickness. Finally, the PM is centered above the coil and embedded by another elastomeric layer.

5. Simulation results and discussion

The numerical simulations are accomplished for two different MEMS actuators, which are varied in the geometric parameters of the used coil and of the PM, respectively. Depending on these results, the impact on the mechanical deformation of the elastomeric layers is numerically investigated.

The first actuator consists of a coil with $N = 6$ windings and a PM, which has with respect to the plane coil surface an orthogonally directed remanent induction $\mathbf{B}_r = [0, 0, 1.42]^T T$. The geometric dimensions can be found in Table I. The acting normal force on the PM is computed with the four mentioned force calculation methods and is compared to the mean value of a series of laboratory measurements. Figure 3 presents the normal force against a variation of the PM/coil-distance in a span of 100-3000 μm. Furthermore, the green data curve (BS_{av}) represents the average normal force of all force calculation methods, which was calculated with the magnetic field values of the coupled FEM/BEM/Biot-Savart approach. Overall, all simulated values show a very good approximation of the measurement data, particular for a PM/coil-distance around 1,000 μm. Some values for this distance are also presented in Table II. For a decreasing distance, it seems that the force calculations of a PM with the equivalent sources methods are clearly more accurate than the MST and VW, respectively. The maximum variance with respect to the measurement data shows the average normal force component calculated with FEM/BEM/Biot-Savart approach. The values show a good sloping curve approximation, but have an average variation of 11.1 percent in a span of 100-1,000 μm compared to the measurement data. A possible reason is the poor approximation of the geometric dimension of the cross-section of the micro-coil. But since this method does not require a finite element discretization of the coil, a memory efficient and faster calculation of the occurring forces can be performed. Furthermore, it should be noted, that all numerical results were not

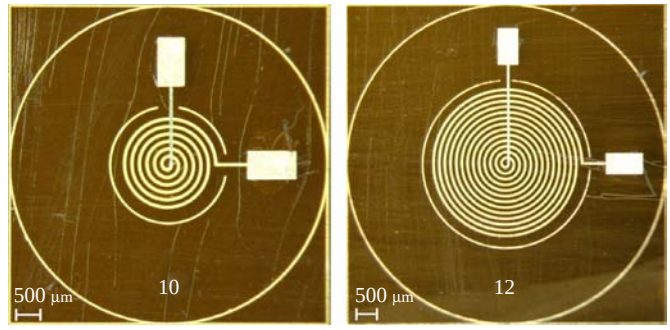

(a) (b)

Figure 2.
(a) Fabricated planar micro-coils with $N = 6$ windings and (b) $N = 13$ windings

Table I.
Different parameters of the first MEMS actuator

Actuator 1	N	$\varnothing$ [μm]	Profile [μm^2]	I [mA]	B_r [T]
Coil	6	1,850	50 × 10	100	–
PM	–	2,000	2,000 × 2,000	–	1.42

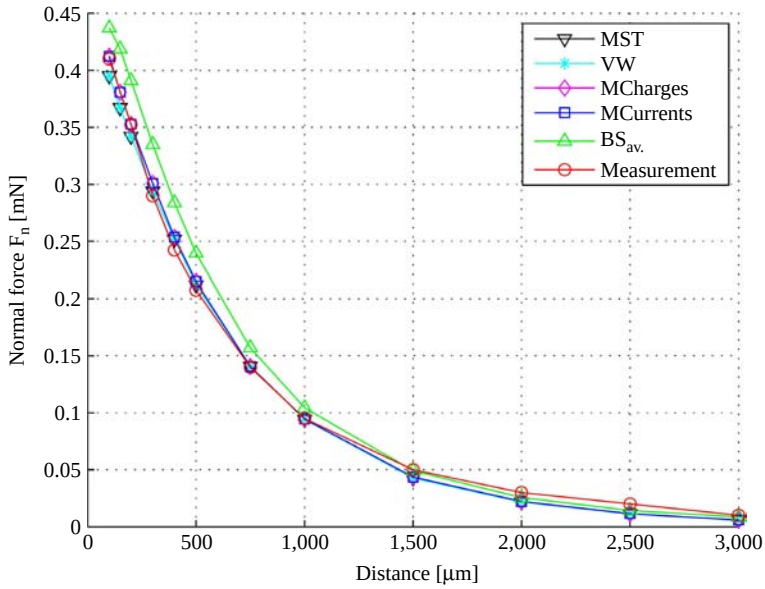

Figure 3.
The measured and simulated normal force component F_n of the first MEMS actuator against the PM/coil distance

compared to analytical ones, but to a mean measurement value, which could be self-affected by material and measurement tolerances.

The second example is a MEMS actuator with $N = 13$ windings and also a PM with a remanent induction $\mathbf{B}_r = [0, 0, 1.42]^T T$. The geometric quantities are deposited in Table III. As in the previous example, the normal force components are shown against the PM/coil-distance in a span of 100-3,000 μm (Figure 4). The different normal forces based on the FEM/BEM approach are almost identically, unlike the tangential force components. An example of the different forces for a distance of $1,000\mu$m is shown in Table IV. The obtained forces with the FEM/BEM/Biot-Savart approach lead again to a good curve approximation, but the differences to the measurement values are larger than the differences of the force values based on the pure FEM/BEM approach. However, due to more windings of the coil, its discretization with finite elements is much more complex than in the previous case. To hold the same accuracy it is necessary to increase the degrees of freedom. In such a case, it is useful to have an

Table II.
Tangential (F_x, F_y) and normal force (F_n) components of the first MEMS actuator at a PM/coil-distance of 1,000 μm. Furthermore, a percentage error (Err_n) with respect to the measurement value of 95.0 μN is denoted

Actuator 1	MST	VW	MCha	MCu	BS$_{av}$
F_x [μN]	−0.9	−1.0	−0.6	−0.6	−0.3
F_y [μN]	4.9	−3.1	6.4	2.4	−4.4
F_n [μN]	94.1	94.1	94.5	94.5	104.3
Err_n [%]	−0.95	−0.95	−0.53	−0.53	9.79

alternative calculation method like the FEM/BEM/Biot-Savart coupled approach to increase the calculation speed and decrease the need of memory storage, while an imprecisely force result is tolerable.

Another investigated aspect is the mechanical behavior of the MEMS actuators. For this reason, based on the previous force calculation a subsequent structural analysis was accomplished. Therefore, a model with the two elastomeric layers was configured with a PM/coil-distance of 1,000 μm. The elastic modulus of the separation layer was set to $E_1 = 0.125\,\text{MPa}$, the other one was set to $E_2 = 1\,\text{MPa}$. An example of the

Table III.
Different parameters of the second MEMS actuator

Actuator 2	N	$\varnothing$ [μm]	Profile [μm^2]	I [mA]	B_r [T]
Coil	13	3,850	50 × 10	100	–
PM	–	3,000	3,000 × 2,000	–	1.42

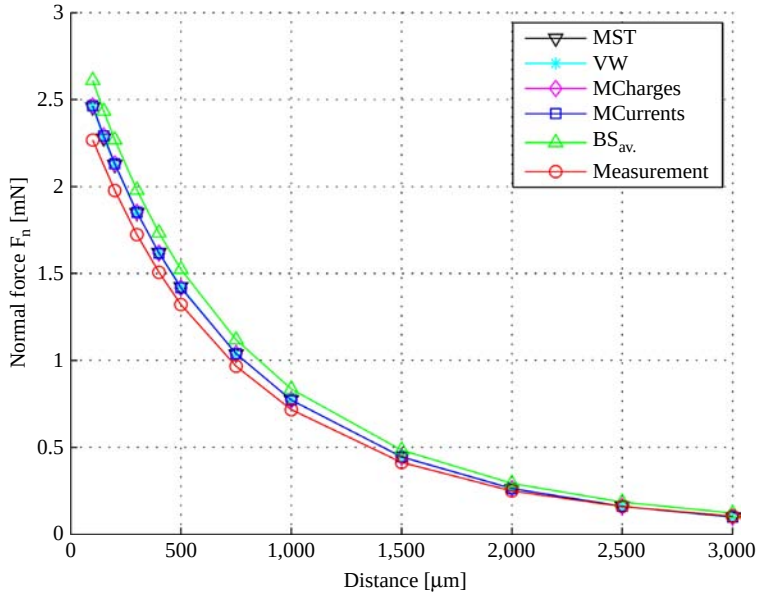

Figure 4.
The measured and simulated normal force component F_n of the second MEMS actuator against the PM/coil distance

Table IV.
Tangential (F_x, F_y) and normal force (F_n) components of the second MEMS actuator at a PM/coil-distance of 1,000 μm. Furthermore, a percentage error (Err_n) with respect to the measurement value of 717 μN is denoted

Actuator 2	MST	VW	MCha	MCu	BS$_{av}$
F_x [μN]	−6.2	3.3	−1.8	−1.0	−0.1
F_y [μN]	6.2	0.5	13.9	3.2	0.0
F_n [μN]	773	773	771	771	835
Err_n [%]	7.8	7.8	7.5	7.5	16.5

configuration for the second actuator and a possible displacement for the case of a repulsive force acting on the PM is shown in Figure 5. The green line on the upper edge of the vertical cut of the MEMS actuator marks the position, where in Figure 6 the local displacements of the elastomeric layer are shown. The first subplot in Figure 6 shows nearly the same material deformation for all implemented force calculation methods. Only the average forces based on the FEM/BEM/Biot-Savart approach lead to higher local displacements. This behavior corresponds to the calculated force values at the distance of 1,000 μm in Figure 4 and Table IV, respectively. Subplot 2 in Figure 6 shows the span of $-2,000 \leq x \leq 2,000$ of subplot 1 in detail to clarify the impact of the different force calculation methods on the mechanical deformation. Corresponding to the values of the tangential force component F_x (Table IV), the PM slightly tilts to one side. The maximum tilt of nearly 0.65 nm results for the forces calculated with the MST. A final conclusion which of the deformation is the best approximation for the real mechanical behavior can only be assumed, because of non-existent measurement values. But due to the slight asymmetry of the planar spiral coil, it seems that the negative directed tangential force values (F_x) are more accurate than the positive (VW) ones. This assumption would also correspond to the tangential force components shown in Table II.

6. Conclusion

In this work, a numerical model of a micrometer scaled actuator was presented. The occurring magnetic interactions inside the MEMS actuator were computed by

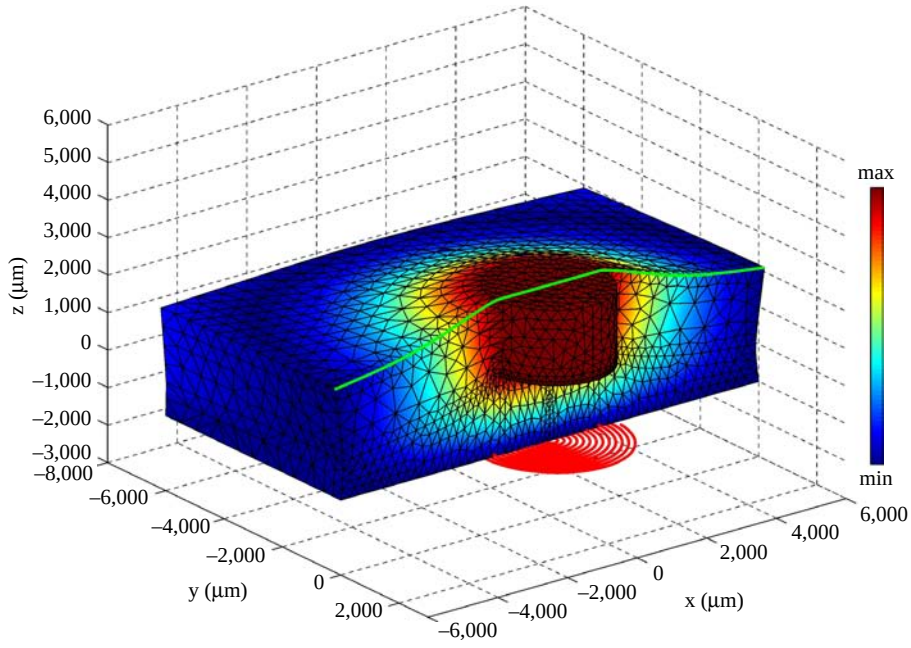

Notes: The red spiral line represents the position of the micro-coil; the green line marks the upper edge of the vertical cut of the model configuration

Figure 5.
An example for the material displacements for the second MEMS actuator

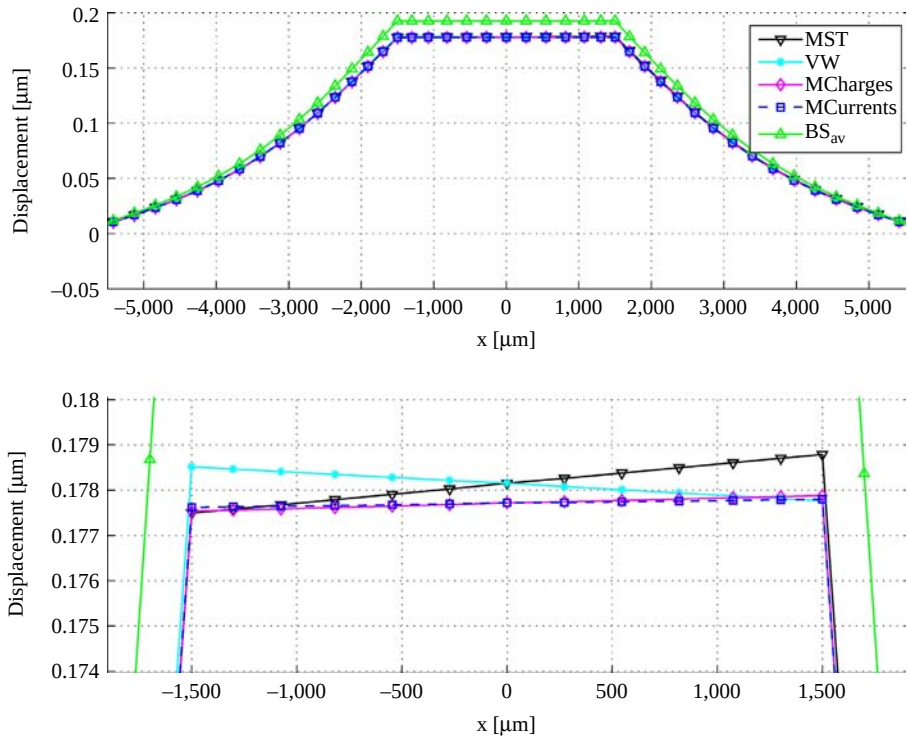

Figure 6.
The first subplot shows the displacements on the marked green line in Figure 5. The second subplot shows the local displacements in a span of $-2{,}000 \leq x \leq 2{,}000$ more detailed

a hybrid FEM/BEM approach and by a coupled FEM/BEM/Biot-Savart approach. With the resulting magnetic field data, the acting forces were calculated with four different methods, i.e. MST, VW and both equivalent magnetic sources methods, and compared to each other and to laboratory measurements. It has been shown that all methods result in a good force approximation, particular for the forces based on the hybrid FEM/BEM approach. For the considered multiscale problem, the main disadvantage of this approach is the large number of finite elements, which are needed to decompose the space of the thin coil. The FEM/BEM/Biot-Savart approach allows the calculation in a memory and time efficient manner, but has less accuracy, due to the poor approximation of the cross-section of the coil. Concerning the different force calculation methods, the forces based on the equivalent magnetic sources show the least variations with respect to the measurement data and the implementation is straightforward. This performance was also reflected by the results of the accomplished subsequent structural analysis.

References

Coulomb, J.L. (1983), "A methodology for the determination of global electromechanical quantities from a finite element analysis and its application to evaluation of magnetic forces, torques and stiffness", *IEEE Transactions on Magnetics*, Vol. 19 No. 6, pp. 2514-19.

de Medeiros, L.H., Reyne, G., Meunier, G. and Yonnet, J.P. (1998), "Distribution of electromagnetic force in permanent magnets", *IEEE Transactions on Magnetics*, Vol. 34 No. 5, pp. 3012-15.

Hefner, J.N. and Bushell, D.M. (1990), *Viscous Drag Reduction in Boundary Layers*, American Institute of Aeronautics and Astronautics, Washington, DC.

Kabashima, T., Kawahara, A. and Goto, T. (1988), "Force calculation using magnetizing currents", *IEEE Transactions on Magnetics*, Vol. 24 No. 1, pp. 451-4.

Kim, D.-H., Lowther, D.A. and Sykulski, J.K. (2005), "Efficient force calculations based on continuum sensitivity analysis", *IEEE Transactions on Magnetics*, Vol. 41 No. 5, pp. 1404-7.

Kurz, S. and Russenschuck, S. (1999), "Accurate calculation of magnetic fields in the end regions of superconducting accelerator magnets using the BEM-FEM coupling method", *Proceedings of the 1999 Particle Accelerator Conference, New York, USA*, pp. 2796-8.

Kurz, S., Fetzer, J. and Lehner, G. (1995), "An improved algorithm for the BEM-FEM-coupling method using domain decomposition", *IEEE Transactions on Magnetics*, Vol. 31 No. 3, pp. 1737-40.

Lee, S.-H., Park, I.-H. and Lee, K.-S. (2000), "Comparison of mechanical deformations due to different force distributions of two equivalent magnetization models", *IEEE Transactions on Magnetics*, Vol. 34 No. 4, pp. 1368-72.

Liu, C. (1998), "Development of surface micromachined magnetic actuators using electroplated permalloy", *Mechatronics*, Vol. 8 No. 5, pp. 613-33.

Melcher, J.R. (1981), *Continuum Electromechanics*, MIT Press, Cambridge, MA.

Preis, K., Bardi, I., Biro, O., Magele, C., Renhart, W., Richter, K.R. and Vrisk, G. (1991), "Numerical analysis of 3D magnetostatic fields", *IEEE Transactions on Magnetics*, Vol. 27 No. 5, pp. 3798-803.

Preisner, T. and Mathis, W. (2009), "A three dimensional FEM-BEM approach for the simulation of magnetic force microscopes", *PIERS Online*, Vol. 5 No. 3, pp. 281-6.

Salon, S.J., Slavik, C.J., DeBortoli, M.J. and Reyne, G. (1995), "Analysis of magnetic vibrations in rotating electric machines", in Ratnajeevan, S. and Hoole, H. (Eds), *Finite Elements, Electromagnetics and Design*, Elsevier Science BV, Amsterdam, pp. 116-78.

Authors' affiliations

Thomas Preisner is based at the Institute of Electromagnetic Theory, Leibniz Universität Hannover, Hannover, Germany.

Christian Bolzmacher is based at EADS Deutschland GmbH, Munich, Germany.

Andreas Gerber is based at the Institute for Materials Science, Christian-Albrechts-Universität zu Kiel, Kiel, Germany.

Karin Bauer is based at EADS Deutschland GmbH, Munich, Germany.

Eckhard Quandt is based at the Institute for Materials Science, Christian-Albrechts-Universität zu Kiel, Kiel, Germany.

Wolfgang Mathis is based at the Institute of Electromagnetic Theory, Leibniz Universität Hannover, Hannover, Germany.

About the authors

Thomas Preisner received his Diploma in Engineering (FH) degree in Electrical Engineering from the University of Applied Sciences in Münster (Germany) in 2005 and the MSc degree in Electrical Engineering and Information Technologies from the Leibniz University of Hannover (Germany) in 2007. Since that time, he has been working as a Research Engineer and Teaching Assistant in the Institute of Electromagnetic Theory at the Leibniz University of Hannover. His main research interests are modeling and simulation of magneto-mechanical systems and

numerical methods applied to electromagnetic fields. Thomas Preisner is the corresponding author and can be contacted at: preisner@tet.uni-hannover.de

Christian Bolzmacher received his Master Degrees from Munich University of Applied Sciences and EPF-Ecole d'Ingenieurs in Mechatronics and Robotics in 2005. After completing his studies, he joined the research laboratories of European aeronautic defence and space company (EADS) Deutschland GmbH in Ottobrunn/Munich, Germany. He developed miniaturized piezoelectric actuators for aeronautic applications and received his PhD degree in 2010 from the Saarland University in Germany and the Ecole Polytechnique, France. His research interests cover smart materials and their characterization especially for microactuators and microsensors.

Andreas Gerber received his PhD in Physics in 2005 from the University of Cologne, Germany for his studies of ferroelectric field-effect-transistors. He spent his post-doc-time at the Center of Advanced European Studies and Research (CAESAR) in Bonn, Germany where he worked on the characterization and fabrication of ferromagnetic-thin-films for high-frequency applications like integrated inductors and dc/dc-converters.

Karin Bauer received her degrees on Experimental and Theoretical Physics from the University of Washington in Seattle and from the University of Regensburg in Germany. She held different functions in research and development in the automotive and aerospace industry and focused later on micro technology for sensing and micro actuation with applications in inertial technology as well as in flow measurement and control. She is now in charge of the micro technology team in the central research entity of the European Aeronautic Defence and Space Company (EADS).

Eckhard Quandt received his Diploma in Physics and his PhD in Engineering at the Technical University Berlin in 1986 and 1990, respectively, working on solid state physics and electron microscopy. For his research and development in this field, he was awarded the "Georg-Sachs-Preis 1995" of the Deutsche Gesellschaft für Materialkunde (DGM). From 2000 to 2006, he was a member of the "Faculty of Mechanical Engineering" at the University of Karlsruhe. Since December 2006, Eckhard Quandt has been a Full Professor and holds the Chair for Inorganic Functional Materials within the Institute for Materials Science at the Faculty of Engineering.

Wolfgang Mathis is a Full Professor at the Leibniz University of Hannover and holds the Chair of the Electromagnetic Theory Group (TET). He is an Institute of Electrical and Electronics Engineers (IEEE) fellow and is currently the Chair of the ITG-FB 8 "Micro- and Nano-electronics" of the German Electrical Engineering Society (VDE/ITG). Furthermore, he is Chair of the IEEE Circuits and Systems Society German chapter since 2001. His main research interests include theory of non-linear circuits and dynamical systems, numerical mathematics, nanoelectronics, quantum computing, analysis and numerics of electromagnetic fields and history of Electrical Engineering and Technical Physics. He has more than 250 publications in journals and books.